Available online at www.sciencedirect.com
ScienceDirect
Journal of Power Sources 179 (2008) 553–559
JOURNAL OF POWER SOURCES
www.elsevier.com/locate/jpowsour

Short communication

A simple and effective process for $Sr_{0.995}Ce_{0.95}Y_{0.05}O_{3-\delta}$ and $BaCe_{0.9}Nd_{0.1}O_{3-\delta}$ solid electrolyte ceramics

Yi-Cheng Liou *, Song-Ling Yang

Department of Electronics Engineering, Kun Shan University, 949, Da Wan Road, Yung-Kang City, Tainan Hsien 71003, Taiwan, ROC

Received 15 November 2007; received in revised form 5 January 2008; accepted 7 January 2008
Available online 16 January 2008

Abstract

A simple and effective reaction-sintering process for $Sr_{0.995}Ce_{0.95}Y_{0.05}O_{3-\delta}$ and $BaCe_{0.9}Nd_{0.1}O_{3-\delta}$ solid electrolyte ceramics was investigated in this study. Without any calcination involved, the mixture of raw materials was pressed and sintered directly. $Sr_{0.995}Ce_{0.95}Y_{0.05}O_{3-\delta}$ ceramics with 98.4% of the theoretical density were obtained after being sintered at 1350 °C for 2 h. A total conductivity 1.42 mS cm^{-1} at 900 °C could be obtained in $Sr_{0.995}Ce_{0.95}Y_{0.05}O_{3-\delta}$ sintered at 1500 °C for 4 h. $BaCe_{0.9}Nd_{0.1}O_{3-\delta}$ ceramics with 91.7% of the theoretical density were obtained after being sintered at 1500 °C for 2 h. A total conductivity 11.54 mS cm^{-1} at 900 °C could be obtained in $BaCe_{0.9}Nd_{0.1}O_{3-\delta}$ sintered at 1350 °C for 6 h. The reaction-sintering process has proven a simple and effective method to obtain useful $Sr_{0.995}Ce_{0.95}Y_{0.05}O_{3-\delta}$ and $BaCe_{0.9}Nd_{0.1}O_{3-\delta}$ ceramics for solid electrolyte applications in solid oxide fuel cells.

Keywords: $SrCeO_3$; $BaCeO_3$; Solid electrolyte; Solid oxide fuel cell; Reaction-sintering process

1. Introduction

Solid oxide fuel cells (SOFCs) transform chemical energy to electrical energy with high conversion efficiency and low pollution. Research and development of SOFCs have received much attention recently [1–4]. There are three parts in an SOFC, including the electrolyte, the anode, and the cathode. A dense electrolyte is needed to prevent gas mixing, whereas the anode and cathode must be porous to allow gas transport to the reaction sites. Iwahara et al. investigated proton conducting perovskite type oxides based on $SrCeO_3$ [5]. $SrCeO_3$ and $BaCeO_3$ doped with certain trivalent rare-earth ions display high conductivity with low activation energy. These compounds have been widely studied and found to be potential materials for applications as solid electrolytes in SOFCs and for applications in steam electrolyses for hydrogen production or as hydrogen sensors [5–15]. Protonic conductivities for these compounds in hydrogen atmosphere are of the order of 10^{-3} to 10^{-2} S cm^{-1} at 600–1000 °C. Sammes et al. reported ionic conductivities of 1 and 7 mS cm^{-1} at 800 °C in $SrCe_{0.95}Y_{0.05}O_{3-\delta}$ and $Sr_{0.995}Ce_{0.95}Y_{0.05}O_{3-\delta}$, respectively. The conductivity of substoichiometric $Sr_{0.995}Ce_{0.95}Y_{0.05}O_{3-\delta}$ is higher than the conductivity of stoichiometric $SrCe_{0.95}Y_{0.05}O_{3-\delta}$ [16]. $BaCe_{0.9}Nd_{0.1}O_{3-\delta}$ ceramics show the highest conductivity, approximately, 5.5×10^{-1} S cm^{-1} at 1000 °C [17]. $SrCeO_3$ and $BaCeO_3$ were usually prepared via solid state reaction route, in which carbonate and oxide of the constituents were mixed and then calcined and sintered at high temperature [5,18,19]. Oxalate coprecipitation technique and modified Pechini process have also been used to obtain these compounds [20,21].

Recently, we prepared $Pb(Mg_{1/3}Nb_{2/3})O_3$ (PMN) and $Pb(Fe_{1/2}Nb_{1/2})O_3$ (PFN) ceramics using a simple and effective reaction-sintering process [22,23]. PbO and Nb_2O_5 were mixed with $Mg(NO_3)_2$ or $Fe(NO_3)_3$ then pressed and sintered directly into PMN and PFN ceramics without any calcination step involved. These are the first successful syntheses of perovskite relaxor ferroelectric ceramics without having to go through the calcination steps in the conventional solid state route or in the columbite process technique. Other Pb-

* Corresponding author. Tel.: +886 6 205 0521; fax: +886 6 205 0250.
E-mail address: ycliou@mail.ksu.edu.tw (Y.-C. Liou).

0378-7753/$ – see front matter © 2008 Elsevier B.V. All rights reserved.
doi:10.1016/j.jpowsour.2008.01.012

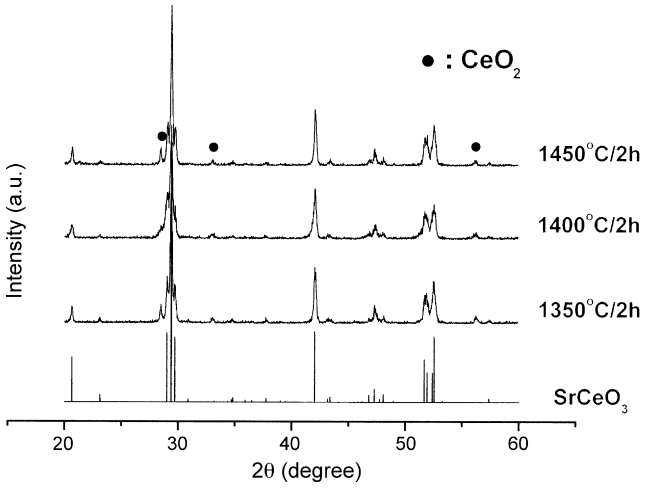

Fig. 1. XRD patterns of SCYO ceramics with 1 wt% B_2O_3 addition.

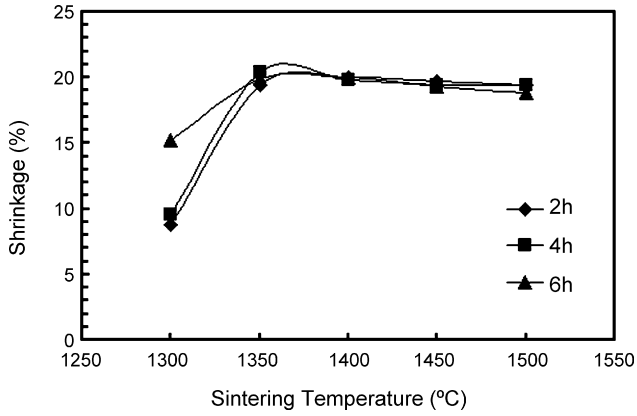

Fig. 2. Shrinkage percentage of SCYO ceramics with 1 wt% B_2O_3 addition sintered at various temperatures and soak time.

based complex perovskite ceramics were also produced by this reaction-sintering process successfully. In our recent studies, some microwave dielectric ceramics such as $BaTi_4O_9$, $(Ba_xSr_{1-x})(Zn_{1/3}Nb_{2/3})O_3$, $Ba_5Nb_4O_{15}$, $Sr_5Nb_4O_{15}$, $CaNb_2O_6$ and $NiNb_2O_6$ were also prepared successfully via this reaction-sintering process [24–28]. In this study, $Sr_{0.995}Ce_{0.95}Y_{0.05}O_{3-\delta}$ and $BaCe_{0.9}Nd_{0.1}O_{3-\delta}$ ceramics prepared using a reaction-sintering process were investigated.

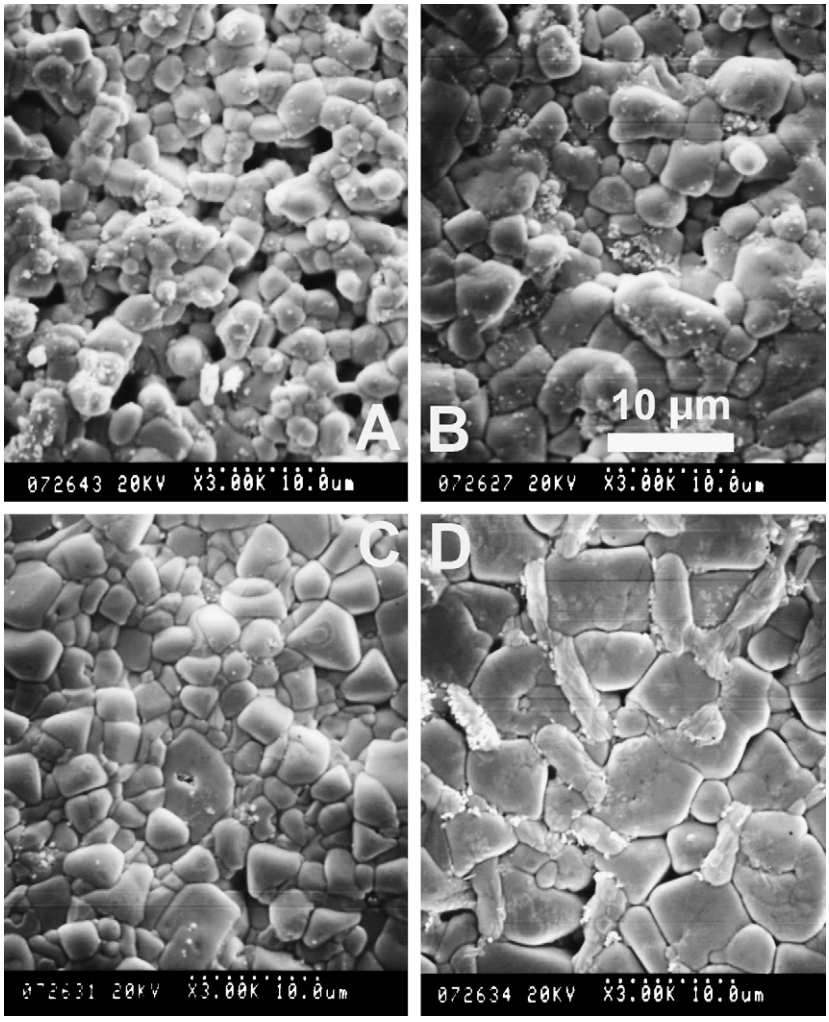

Fig. 3. SEM photographs of SCYO ceramics with 1 wt% B_2O_3 addition sintered at (A) 1300 °C, (B) 1350 °C, (C) 1400 °C, and (D) 1450 °C for 2 h.

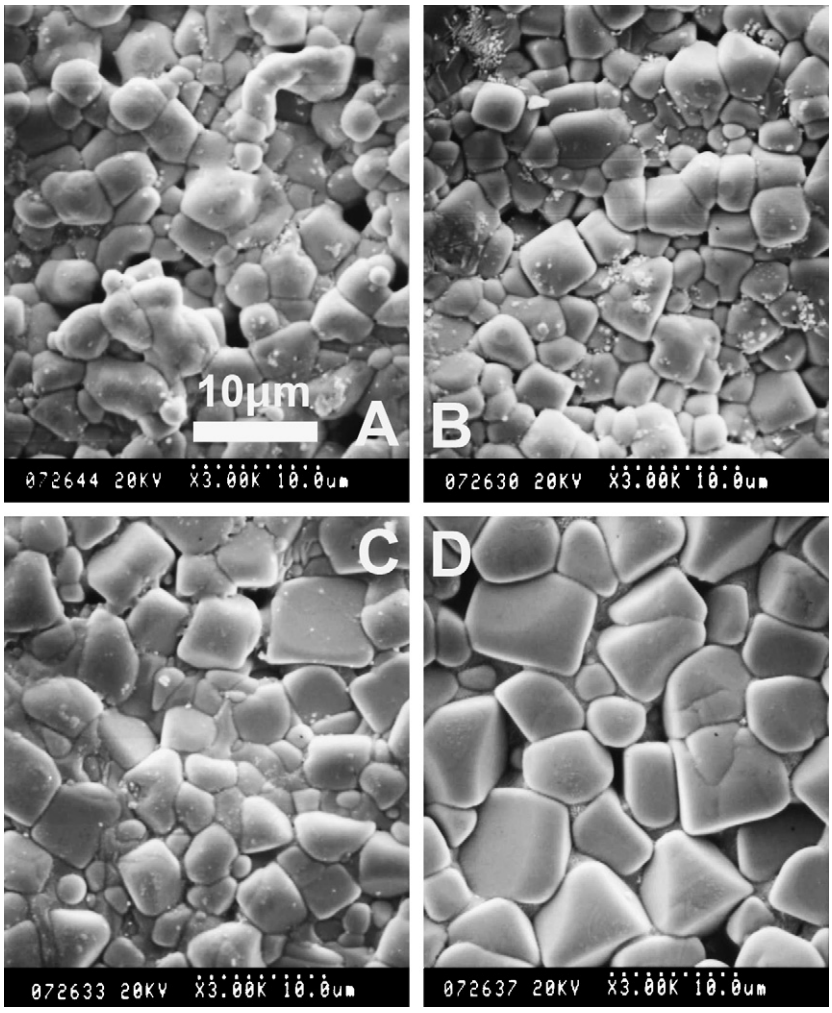

Fig. 4. SEM photographs of SCYO ceramics with 1 wt% B_2O_3 addition sintered at (A) 1300 °C, (B) 1350 °C, (C) 1400 °C, and (D) 1450 °C for 6 h.

2. Experimental

$Sr_{0.995}Ce_{0.95}Y_{0.05}O_{3-\delta}$ (SCYO) and $BaCe_{0.9}Nd_{0.1}O_{3-\delta}$ (BCNO) in this study were prepared from submicron reagent-grade powders: $BaCO_3$ (99.8%, J.T. Baker), $SrCO_3$ (99%, Alfa Aesar), CeO_2 (99.9%, SHOWA), Y_2O_3 (99.9%, Strem Chemicals) and Nd_2O_3 (99.9%, Strem Chemicals). One weight percentage of B_2O_3 (99.9%, NOAH) was added as a sintering aid to lower the sintering temperature. Appropriate amounts of raw materials were milled in acetone with zirconia balls for 12 h. After they had been dried and pulverized, they were formed into pellets 12 mm in diameter and 2–3 mm thick. The pellets were then heated at a rate 10 °C min^{-1} and sintered in a covered alumina crucible at temperatures ranging between 1300 and 1500 °C for 2–6 h in air.

We analyzed the sintered pellets using X-ray diffraction (XRD, D/max-2550/pc, Rigaku, Japan) to check the reflections of the phases. Microstructures were analyzed using scanning electron microscopy (SEM, S-2500, Hitachi, Japan). The density of the sintered pellets was measured using the Archimedes method. Pt-paste was painted on both sides of the sintered and polished pellets and fired at 950 °C for 30 min. The total conductivity was measured using a 2-probe dc method with a 1 mA current source applied. An Agilent 24970A Data Acquisition/Switch Unit was used.

3. Results and discussion

XRD profiles of SCYO ceramics sintered at 1350–1450 °C are illustrated in Fig. 1. These reflections match with those of $SrCeO_3$ in ICDD PDF # 01-081-0026. This proves the perovskite phase SCYO could be obtained via the reaction-sintering process. This simple process is effective not only in preparing $BaTi_4O_9$, $(Ba_xSr_{1-x})(Zn_{1/3}Nb_{2/3})O_3$, $Ba_5Nb_4O_{15}$, $Sr_5Nb_4O_{15}$ and Pb-based complex perovskite ceramics but also effective in preparing perovskite SCYO ceramics. Weak reflections of CeO_2 were also detected in the profile. Liu et al. reported $SrCe_{0.95}Yb_{0.05}O_{3-\delta}$ powders prepared by ethylenediaminetetraacetic acid (EDTA) and citric acid methods were composed of carbonates ($SrCO_3$) and oxides (CeO_2) after being calcined at 400, 600 and 700 °C. However, the XRD spectra of $SrCe_{0.95}Yb_{0.05}O_{3-\delta}$ powders prepared by the glycine method indicate that cubic perovskite $SrCe_{0.95}Yb_{0.05}O_{3-\delta}$, CeO_2, and $SrCO_3$ phases coexist. After sintering at 800 and 900 °C, the

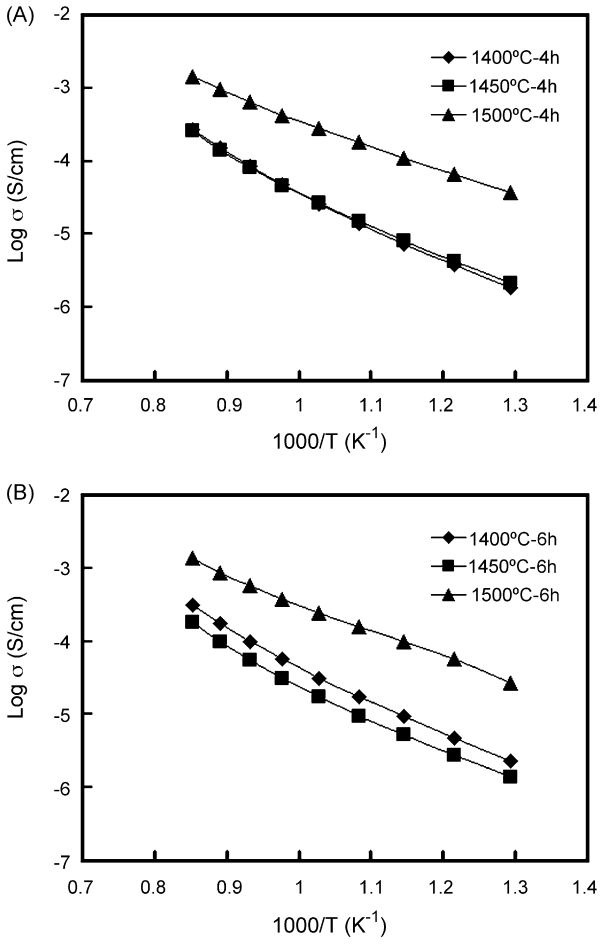

Fig. 5. Total conductivity of SCYO ceramics with 1 wt% B_2O_3 addition sintered at various temperatures for (A) 4 h and (B) 6 h.

XRD patterns of powders prepared by these three methods display the existence of $SrCe_{0.95}Yb_{0.05}O_{3-\delta}$, CeO_2, and SrO crystal phases and the disappearance of $SrCO_3$ phases. At sintering temperature above 950 °C, only the cubic perovskite phase of $SrCe_{0.95}Yb_{0.05}O_{3-\delta}$ was detected [29]. $SrCO_3$ or SrO phases were not detected in SCYO ceramics prepared using the reaction-sintering process in this study.

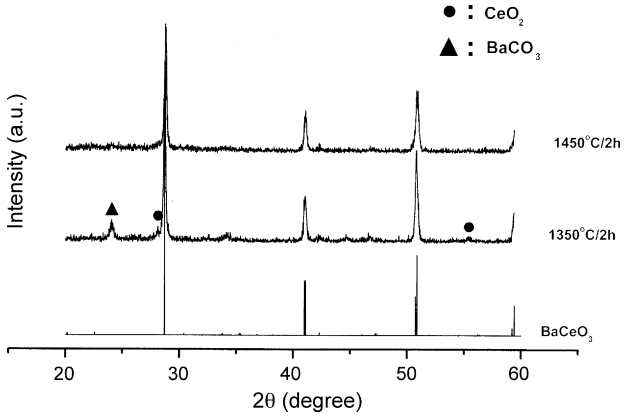

Fig. 6. XRD patterns of BCNO ceramics with 1 wt% B_2O_3 addition.

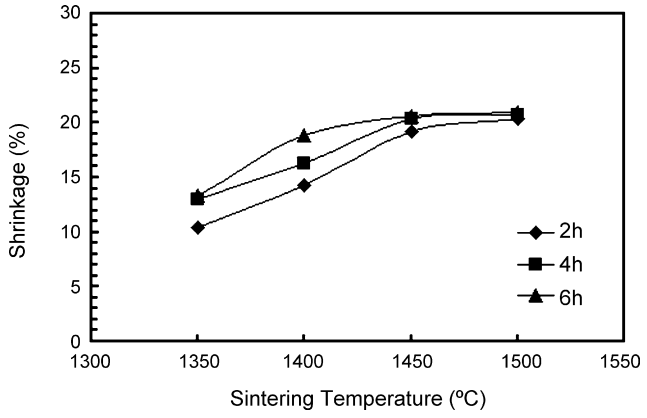

Fig. 7. Shrinkage percentage of BCNO ceramics with 1 wt% B_2O_3 addition sintered at various temperatures and soak time.

The shrinkage percentage of SCYO pellets increased from 1300 °C and saturated at temperatures above 1350 °C as shown in Fig. 2. The density of SCYO ceramics increased with sintering temperature and reached a maximum value 5.69 g cm^{-3} (98.4% of the theoretical value) at 1350 °C/2 h then decreased. A dense electrolyte is needed to prevent gas mixing. Sammes et al. reported a density close to 97% of the theoretical value was obtained in $SrCe_{0.95}Y_{0.05}O_{3-\delta}$ ceramics calcined at 1000 °C/0.5 h and 1300 °C/1 h then sintered at 1500 °C for 11 h [16]. Therefore, the reaction-sintering process is effective to produce SCYO ceramics with high density at a lower sintering temperature although the calcination was bypassed. The SEM photos of SCYO ceramics sintered at 1300–1450 °C for 2 h are shown in Fig. 3. Grains of 2–4 μm were found at 1300 °C and grain growth increased significantly with the sintering temperature. In Fig. 4, larger grains are found in 6 h sintered pellets. Five to ten micrometers of grains could be easily found in 1450 °C sintered pellets.

The total conductivity of SCYO ceramics measured in a temperature range 500–900 °C are shown in Fig. 5. Similar values are obtained in 1400 and 1450 °C sintered SCYO due to similar density and grain size. Higher conductivity is found in 1500 °C sintered SCYO because of the larger grain size. A total conductivity 1.42 mS cm^{-1} ($\log\sigma = -2.848$) at 900 °C could be obtained in SCYO sintered at 1500 °C for 4 h. Iwahara found 5 mS cm^{-1} at 800 °C in hydrogen atmosphere and 1 mS cm^{-1} at 900 °C in 5% hydrogen atmosphere in SCYO [17]. Sammes et al. reported an ionic conductivity around 1 mS cm^{-1} at 800 °C and $P_{H_2O} = 0.01$ atm was obtained in $SrCe_{0.95}Y_{0.05}O_{3-\delta}$ ceramics calcined at 1000 °C/0.5 h and 1300 °C/1 h then sintered at 1500 °C for 11 h [16]. Dionysiou et al. found a total conductivity 0.0557 mS cm^{-1} at 900 °C in 20% O_2 + 80% N_2 atmosphere for $SrCe_{0.95}Tb_{0.05}O_{3-\delta}$ prepared via the citrate method [30]. While in $SrCe_{0.95}Yb_{0.05}O_{3-\delta}$, Kosacki and Tuller obtained $\log\sigma$ in a range from −3 to −2.3 at 900 °C and $P_{O_2} = 10^{-10} \sim 10^{0}$ atm [31]. Activation energy (E_a) of SCYO ceramics calculated from the slope in Fig. 5 are listed in Table 1. In the temperature range 800–900 °C, E_a decreased from 130–133 kJ mol^{-1} in 1400–1450 °C sintered SCYO to 93–99 kJ mol^{-1} in 1500 °C sintered SCYO. It is also

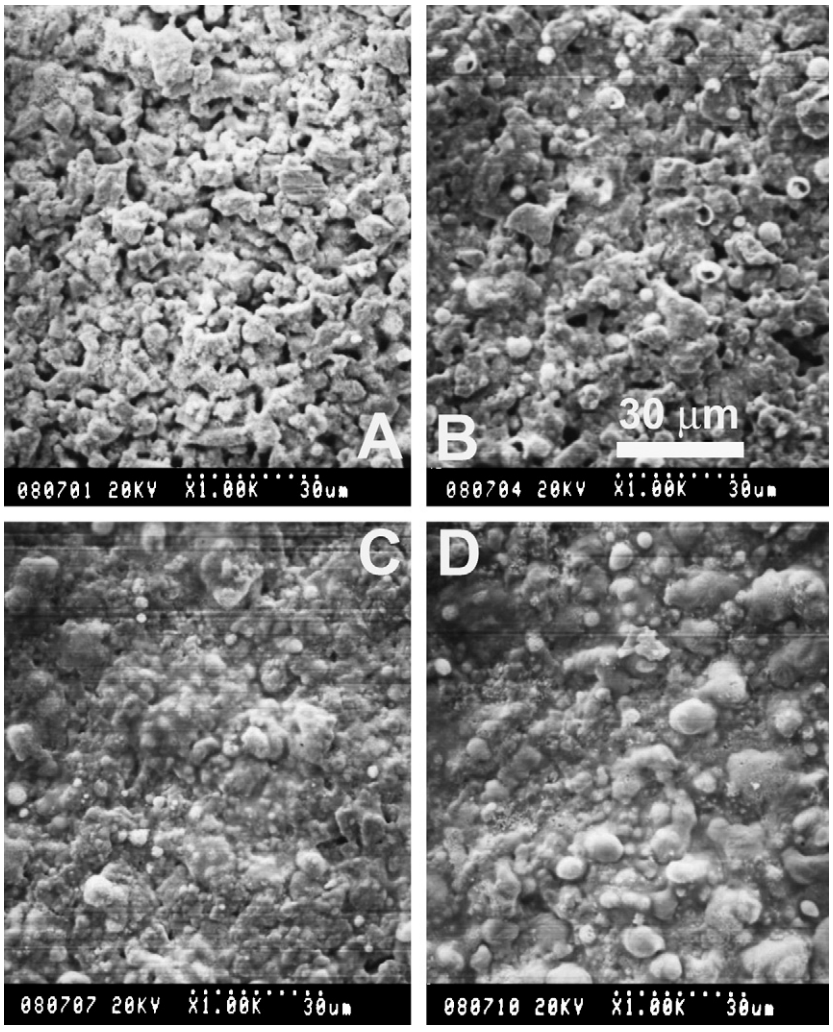

Fig. 8. SEM photographs of BCNO ceramics with 1 wt% B_2O_3 addition sintered at (A) 1350 °C, (B) 1400 °C, (C) 1450 °C, and (D) 1500 °C for 2 h.

noted that E_a is 7–13 kJ mol^{-1} lowered in a lower temperature range 700–900 °C. Similar results were also observed in $SrCeO_3$ doped with 5 mol% of Yb reported by Kumar. E_a decreased from 0.88 eV in 800–1000 °C to 0.55 eV in 327–800 °C for a P_{H_2O} value of 0.023 atm in air [32]. Vries reported $E_a = 64$ kJ mol^{-1} in dry and pure N_2 and $E_a = 91$ kJ mol^{-1} in dry and 100% O_2 in $SrCe_{0.95}Yb_{0.05}O_{3-\delta}$ [33]. Bonanos and Mogensen found $E_a = 110$ kJ mol^{-1} in $Sr_{0.995}Ce_{0.95}Y_{0.05}O_{2.975}$ at 800 °C [34]. The reaction-sintering process has proven a simple and effective method to obtain useful $Sr_{0.995}Ce_{0.95}Y_{0.05}O_{3-\delta}$ ceramics for solid electrolyte applications in solid oxide fuel cells.

Table 1
Activation energy of $Sr_{0.995}Ce_{0.95}Y_{0.05}O_{3-\delta}$ ceramics

Sintering temperature/duration	E_a (kJ mol^{-1}) (eV) (800–900 °C)	E_a (kJ mol^{-1}) (eV) (700–900 °C)
1400 °C/4 h	131.3 (1.36)	121.2 (1.26)
1450 °C/4 h	129.8 (1.35)	116.5 (1.21)
1500 °C/4 h	93.1 (0.97)	86.1 (0.89)
1400 °C/6 h	129.7 (1.34)	118.3 (1.23)
1450 °C/6 h	133.1 (1.38)	120.5 (1.25)
1500 °C/6 h	99.6 (1.03)	89.7 (0.93)

The XRD patterns of BCNO ceramics produced using the reaction-sintering process is shown in Fig. 6. The $BaCeO_3$ phase formed as a major phase and some weak peaks of remained $BaCO_3$ and CeO_2 were also detected in pellets sintered at 1350 °C/2 h. Single phase BCNO ceramic was obtained after sintered at 1450 °C for 2 h. Reaction-sintering process is again proven effective in producing $BaCeO_3$-based ceramics. In BCNO studied by Chen et al., they found the decomposition of $BaCO_3$ and the formation of the perovskite phase take place at about 900 °C and finish completely below 1200 °C from the DTA-TG curves at a heating rate 2 °C min^{-1} [35]. Therefore, the remained $BaCO_3$ and CeO_2 in Fig. 6 may exist due to the fast heating rate 10 °C min^{-1}.

The shrinkage results for BCNO ceramics are shown in Fig. 7. The shrinkage increased with the increase of sintering temperature and soak time. Sintering at 1450 °C is high enough for densification and a shrinkage of 21% is found in 1500 °C/6 h sintered pellets. The density of BCNO ceramics increase with the sintering temperature with the trend observed in Fig. 7. A maximum density 5.82 g cm^{-3} (91.7% of the theoretical value) was obtained at 1500 °C/2 h. In the study of Lu and Jonghe, 6.02 g cm^{-3} was obtained after calcining at 1100 °C for 2 h and

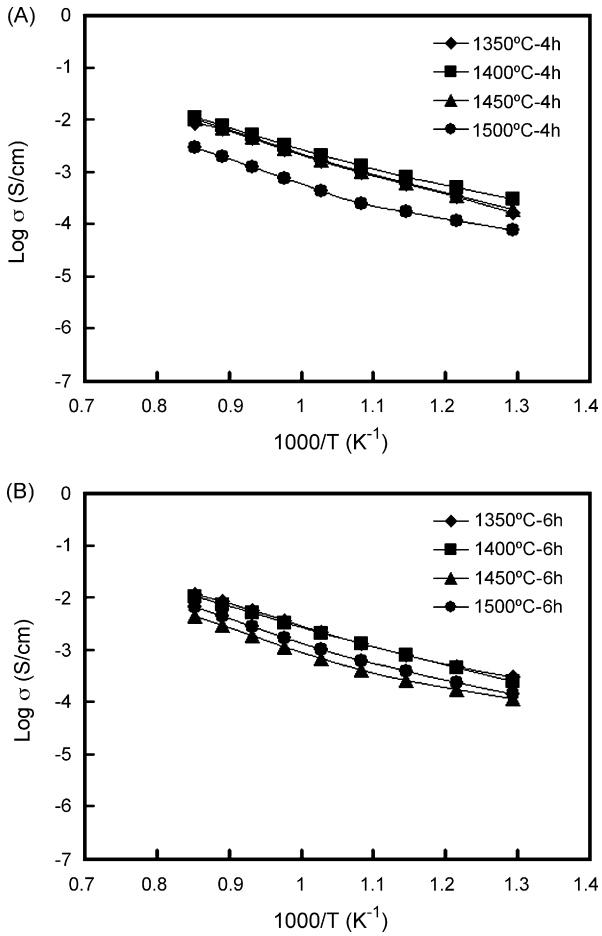

Fig. 9. Total conductivity of BCNO ceramics with 1 wt% B_2O_3 addition sintered at various temperatures for (A) 4 h and (B) 6 h.

sintering at 1500 °C for 2 h [36]. It is found that dense pellets could be obtained easier in SCYO than in BCNO via the reaction-sintering process. The SEM photos of BCNO ceramics sintered at 1350–1500 °C for 2 h are shown in Fig. 8. Porous pellets are seen in 1350 and 1400 °C sintered BCNO. Dense pellets are observed in 1450 and 1500 °C sintered BCNO. In pellets sintered for 4 and 6 h, similar morphology are observed and porous pellets are seen only in 1350 °C sintered BCNO. The morphology in Fig. 8 is similar to $BaCe_{0.9}Sm_{0.1}O_{3-\delta}$ and $BaCe_{0.8}Gd_{0.1}Sm_{0.1}O_{3-\delta}$ ceramics synthesized by the sol–gel method [37].

Fig. 9 shows the total conductivity of BCNO ceramics measured in a temperature range 500–900 °C. The total conductivity for 1350 °C/4 h sintered BCNO are close to 1450 °C/4 h sintered BCNO. Lower values are found in 1500 °C/4 h sintered pellets. A total conductivity 11.01 mS cm^{-1} ($\log\sigma = -1.958$) could be obtained at 900 °C in 1400 °C/4 h sintered BCNO. For 6 h sintering pellets, 11.54 mS cm^{-1} ($\log\sigma = -1.938$) could be obtained at 900 °C in 1350 °C sintered BCNO. Iwahara found 33 mS cm^{-1} in BCNO at 900 °C in hydrogen atmosphere [17]. Chen et al. reported $\ln(\sigma T) \sim 1.555$ kS cm^{-1} around 740 °C in dry air was obtained in BCNO ceramics [38]. In Fig. 9, $\ln(\sigma T) = 1.307$ kS cm^{-1} at 750 °C in air was obtained. Activation energy of BCNO ceramics calculated from the slope in Fig. 9 are listed in Table 2. In the temperature range 800–900 °C, E_a increased from 80.8–81.5 kJ mol^{-1} in 1350 °C sintered BCNO to 96.4–98.8 kJ mol^{-1} in 1500 °C sintered BCNO. E_a remains almost the same in 1400–1500 °C sintered BCNO. While in 1350 °C sintered BCNO, it raised 6.5–7 kJ mol^{-1} in a lower temperature range 700–900 °C. Ryu and Haile reported $E_a = 0.58$ eV in dry argon and $E_a = 0.61$ eV in H_2O-saturated argon in 100–400 °C in BCNO ceramics calcined at 1350 °C/10 h and 1500 °C/12 h then sintered at 1650 °C/12 h in air [39]. Chen et al. observed $E_a = 47.6$, 48.2, and 49.1 kJ mol^{-1} in hydrogen atmosphere in 500–800 °C in BCNO ceramics prepared through oxalate coprecipitation, carbonate-oxide mixed by ball-milling and carbonate-oxide mixed by mortar/pestle, respectively [35]. The reaction-sintering process has proven a simple and effective method to obtain useful BCNO ceramics for solid electrolyte applications in solid oxide fuel cells.

Table 2
Activation energy of $BaCe_{0.9}Nd_{0.1}O_{3-\delta}$ ceramics

Sintering temperature/duration	E_a (kJ mol^{-1}) (eV) (800–900 °C)	E_a (kJ mol^{-1}) (eV) (700–900 °C)
1350 °C/4 h	80.8 (0.84)	87.8 (0.91)
1400 °C/4 h	87.8 (0.91)	87.4 (0.91)
1450 °C/4 h	93.2 (0.97)	94.4 (0.98)
1500 °C/4 h	98.8 (1.02)	99.3 (1.03)
1350 °C/6 h	81.5 (0.84)	88.0 (0.91)
1400 °C/6 h	86.6 (0.90)	86.4 (0.90)
1450 °C/6 h	95.4 (0.99)	96.8 (1.00)
1500 °C/6 h	96.4 (1.00)	96.0 (1.00)

4. Conclusions

Reaction-sintering process can efficiently transform the mixture of raw materials into $Sr_{0.995}Ce_{0.95}Y_{0.05}O_{3-\delta}$ and $BaCe_{0.9}Nd_{0.1}O_{3-\delta}$ ceramics although the calcination stage is bypassed. $Sr_{0.995}Ce_{0.95}Y_{0.05}O_{3-\delta}$ ceramics with 98.4% of the theoretical density were obtained after being sintered at 1350 °C for 2 h. A total conductivity 1.42 mS cm^{-1} at 900 °C could be obtained in $Sr_{0.995}Ce_{0.95}Y_{0.05}O_{3-\delta}$ sintered at 1500 °C for 4 h. Single phase $BaCe_{0.9}Nd_{0.1}O_{3-\delta}$ ceramic could be obtained at 1450 °C/2 h sintering. $BaCe_{0.9}Nd_{0.1}O_{3-\delta}$ ceramics with 91.7% of the theoretical density were obtained after being sintered at 1500 °C for 2 h. A total conductivity 11.54 mS cm^{-1} at 900 °C could be obtained in $BaCe_{0.9}Nd_{0.1}O_{3-\delta}$ sintered at 1350 °C for 6 h. The reaction-sintering process has proven a simple and effective method to obtain useful $Sr_{0.995}Ce_{0.95}Y_{0.05}O_{3-\delta}$ and $BaCe_{0.9}Nd_{0.1}O_{3-\delta}$ ceramics for solid electrolyte applications in solid oxide fuel cells.

References

[1] N.Q. Minh, Chemtech 21 (1991) 120–126.
[2] T. Yoshida, T. Hoshina, I. Mukaizawa, S. Sakurada, J. Electrochem. Soc. 136 (1989) 2604–2606.
[3] A.V. Virkar, J. Electrochem. Soc. 138 (1991) 1481–1487.
[4] N.Q. Minh, J. Am. Ceram. Soc. 76 (1993) 563–588.
[5] H. Iwahara, T. Esaka, H. Uchida, N. Maeda, Solid State Ionics 3/4 (1981) 359–363.

[6] H. Uchida, N. Maeda, H. Iwahara, Solid State Ionics 11 (1983) 117–124.
[7] H. Iwahara, Solid State Ionics 28–30 (1988) 573–578.
[8] N. Bonanos, K.S. Knight, B. Ellis, Solid State Ionics 79 (1995) 161–170.
[9] H. Iwahara, H. Uchida, K. Ogaki, H. Nagato, J. Electrochem. Soc. 138 (1991) 295–299.
[10] N. Bonanos, B. Ellis, M.N. Mahmood, Solid State Ionics 28–30 (1988) 579–584.
[11] W.T. Lian, L.Z. Yi, X. Zhihong, J. Mater. Sci. Lett. 13 (1994) 1032–1034.
[12] M.K. Paria, H.S. Maiti, Solid State Ionics 13 (1984) 285–292.
[13] H. Iwahara, H. Uchida, K. Ono, K. Ogako, J. Electrochem. Soc. 135 (1988) 529–533.
[14] J.F. Liu, A.S. Nowick, Solid State Ionics 50 (1992) 131–138.
[15] D.A. Stevenson, N. Jiang, R.M. Buchanan, F.E.G. Henn, Solid State Ionics 62 (1993) 279–285.
[16] N. Sammes, R. Phillips, A. Smirnova, J. Power Sources 134 (2004) 153–159.
[17] H. Iwahara, Solid State Ionics 86–88 (1996) 9–15.
[18] T. Scherban, R. Villeneuve, L. Abello, G. Lucazeau, Solid State Ionics 61 (1993) 93–98.
[19] R.C.T. Slade, N. Singh, Solid State Ionics 46 (1991) 111–115.
[20] S.D. Flint, R.C.T. Slade, Solid State Ionics 77 (1995) 215–221.
[21] M.J. Scholten, J. Schoonman, J.C. van Miltenburg, H.A.J. Oonk, Solid State Ionics 61 (1993) 83–91.
[22] Y.C. Liou, K.H. Tseng, Mater. Res. Bull. 38 (2003) 1351–1357.
[23] Y.C. Liou, C.Y. Shih, C.H. Yu, Mater. Lett. 57 (2003) 1977–1981.
[24] Y.C. Liou, C.T. Wu, K.H. Tseng, T.C. Chung, Mater. Res. Bull. 40 (2005) 1483–1489.
[25] Y.C. Liou, J.H. Chen, H.W. Wang, C.Y. Liu, Mater. Res. Bull. 41 (2006) 455–460.
[26] Y.C. Liou, W.H. Shiue, C.Y. Shih, Mater. Sci. Eng. B 131 (2006) 142–146.
[27] Y.C. Liou, M.H. Weng, C.Y. Shiue, Mater. Sci. Eng. B 133 (2006) 14–19.
[28] Y.C. Liou, C.Y. Shiue, Mater. Res. Soc. Symp. Proc. 848 (2005) 115–119.
[29] S. Liu, X. Tan, K. Li, R. Hughes, Ceram. Int. 28 (2002) 327–335.
[30] D. Dionysiou, X. Qi, Y.S. Lin, G. Meng, D. Peng, J. Membr. Sci. 154 (1999) 143–153.
[31] I. Kosacki, H.L. Tuller, Solid State Ionics 80 (1995) 223–229.
[32] R.V. Kumar, J. Alloys Compd. 408–412 (2006) 463–467.
[33] K.J. de Vries, Solid State Ionics 100 (1997) 193–200.
[34] N. Bonanos, M. Mogensen, Solid State Ionics 97 (1997) 483–488.
[35] F.L. Chen, O.T. Sørensen, G.Y. Meng, D.K. Peng, Solid State Ionics 100 (1997) 63–72.
[36] C.H. Lu, L.C.D. Jonghe, J. Am. Ceram. Soc. 77 (1994) 2523–2528.
[37] Z.J. Li, R.Q. Liu, J.D. Wang, Z. Xu, Y.H. Xie, B.H. Wang, Sci. Technol. Adv. Mater. 8 (2007) 566–570.
[38] F.L. Chen, O.T. Sørensen, G.Y. Meng, D.K. Peng, J. Eur. Ceram. Soc. 18 (1998) 1389–1395.
[39] K.H. Ryu, S.M. Haile, Solid State Ionics 125 (1999) 355–367.